Journal of Materials Chemistry A

Accepted Manuscript

ROYAL SOCIETY OF CHEMISTRY

www.rsc.org/materialsA

Flexible full-solid state supercapacitor based on zinc sulfide spheres growing on carbon textile with superior charge storage

Muhammad Sufyan Javed[a,b], Jie Chen[a], Lin Chen[a], Yi Xi[a], Cuilin Zhang[a], Buyong Wan[a], Chenguo Hu[a]*

[a]*Department of Applied Physics, Chongqing University, Chongqing 400044, P. R. China*

[b]*Department of Physics, COMSATS Institute of Information Technology Lahore 54000, Pakistan*

[*]*Corresponding author. Tel: +86 23 65670880; Fax: +86 23 65678362*

E-mail address: hucg@cqu.edu.cn (CG Hu)

Abstract

Nowadays, it is essential for us to design and fabricate efficient and cost-effective electrode materials for energy conversion and storage systems. Nanostructures are remarkable electrode materials for their high surface area and large number of active sites. Herein zinc sulfide (ZnS) nanospheres with large surface area which hydrothermally grow on a flexible carbon textile (CT). The specific area and porosity is analyzed in detail under different pressures. The electrode based on the ZnS assembled CT (ZnS-CT) exhibits high capacitance of 747 F g^{-1} at scan rate of 5 m Vs^{-1} in LiCl aqueous electrolyte. The ZnS-CT is directly used as binder free electrodes for the fabrication of the symmetric flexible full solid state supercapacitor. The ZnS-CT supercapacitor shows excellent electrochemical performance along with light weight, thinness and good flexibility. The ZnS-CT supercapacitor demonstrates good capacitive behavior with high specific capacitance of 540 F g^{-1} (areal capacitance of 56.25 F cm^{-2}) at scan rate of 5 m Vs^{-1} with good rate capability and excellent cycling stability (94.6 % retention of initial capacitance after 5000 cycles) at constant current density of 0.8 mA cm^{-2}. The high energy density of 51 Wh kg^{-1} at power density of 205 W kg^{-1} is achieved, indicating excellent ions accessibility and charge storage ability. Furthermore, three charged supercapacitors connected in series can light 4 red color light emitting diodes (2.0 V, 15 mA) for 2 min. ZnS nanospheres with large specific surface area combined with flexible carbon textile substrate offers a promising material in energy storage devices with high energy.

Keywords: Zinc sulfide, carbon textile, nanospheres, flexible, supercapacitor

1. Introduction

Supercapacitors, also known as electrochemical capacitors, are considered as one of the promising and reliable devices in the field of energy storage system due to their high power density, long lifetime, quick charging and environmental friendliness.[1-3] Recently flexible electronics have attracted more attention due to their potential applications in portable, wearable and roll up displays. Several kinds of functional devices have been developed such as thin film transistors, photodetectors, energy conversion and storage devices including fuel cells, solar cells, nanogenerators, lithium-ion batteries and supercapacitors. All electronic devices require light, flexible, long-life and cost-effective energy storage systems with high energy and power densities.[4] However, the conventional energy storage devices, such as batteries, cannot fulfill the requirements of energy for next generation electronic devices with small size, light weight and flexibility. Therefore supercapacitors have been used in many portable devices and heavy vehicles. Currently supercapacitors are based on carbon materials (graphene, carbon aerogels) for the double layer capacitance,[5] while composites of carbon and conductive polymers,[6] transition metal oxides[7] (TMO) and transition metal chalcogenides[8] (TMCs) for the combination of double layer capacitance with Faradic redox pseudocapacitance which shows considerably higher specific capacitance as compared with carbon based supercapacitors. TMOs and TMCs are especially investigated as promising electrode materials for next generation supercapacitors due to their multiple oxidation states for generation of pseudocapacitance.[9] Therefore, it is a great challenge to enhance the electrochemical performance of pseudocapacitive materials by controlling their structure, morphology, surface area.[10] In recent years, TMCs are reported to have been electrochemically active materials and some exhibit higher electrochemical performance than single component oxides and carbon based materials due to their oxidation

states and high electrical conductivity such as cupper sulfide (Cu_7S_4),[11] potassium cupper selenium (KCuSe),[12] molybdenum sulfide (MoS_2),[13] nickel sulfide (NiS_2),[14] cobalt sulfide (Co_9S_8),[15] and tungsten sulfide (WS_2).[16] TMCs have been considered as reliable and promising alternative electrode materials for next generation pseudocapacitors with several advantages, such as low cost, high conductivity, abundance in nature and environmental friendliness.[17]

Zinc oxide (ZnO) and zinc sulfide (ZnS) are two wide band gap multifunctional semiconductors and extensively studied in nanogenerators, sensors, lasers, photodetectors, transistors, photocatalysis and piezotronics due to good electrical conductivity, electronic properties, stability and wide range of morphological properties.[18-20] Wang et al. reported rectangular porous ZnS nanotubes and ZnO/ZnS nanocables for photoluminescence properties.[21] Zhang et al. reported hybrid ZnO/ZnS nanoforests as an electrode material for solid state supercapacitor with areal capacitance of 217 mF cm^{-2} in 1 M KOH aqueous solution and 82 % capacitance retention after 2000 cycles.[22] However, the heterostructure of the ZnO/ZnS nanoforests would have extra barriers for the electron transmission between the interfaces which limits the achievement of a high areal capacitance. Improvement of the charge storage based on the ZnS material with a specific structure and contact directly to electron collector is still a challenging work.

For real applications of flexible supercapacitors, particular attention should be paid to the mechanical, electrical, electrochemical and interfacial properties of the electrodes. Currently remarkable attention has been paid to the rational design and materials directly growing on conductive substrate with unique architecture to achieve high electrochemical, electrical, optical and mechanical properties.[23] Several types of conductive substrates have been used as current collector to enhance the electrochemical performance of supercapacitors such as carbon fiber papers,[4, 24] graphene sheets,[5, 25] nickel foam,[23, 26] copper foam[27] and carbon textiles.[11, 13, 28]

Among these substrates carbon textile is considered as an ideal flexible and conductive substrate for directly growing active material due to good mechanical strength, flexibility, excellent conductivity and low cost. Generally, the active materials are deposited or coated on carbon textile substrates and then used as electrodes for supercapacitors, which may contain binders, conductive agent and active material. In this case part of electroactive sites of the active material could not contact the electrolyte due to the use of binder and conductive agents. The binder will reduce the deep penetration of electrolyte ions into the electrode materials and hinder the performance of the supercapacitors.[29] It is essential to design the rational architectures of electrodes for supercapacitor. Recently, an attractive way is to directly grow nanostructures of different binary materials on conductive substrates without use of binder. Direct growth method has some intrinsic advantages, such as good electrical conductivity, low diffusion resistance, fast electron transportation and deep electrolyte ion penetration.

Herein, we report for the first time the ZnS nanospheres growing directly on flexible carbon textile (ZnS-CT) via a simple and cost effective hydrothermal method with high specific surface area. The ZnS-CT electrode exhibits high capacitance of 747 F g^{-1} at scan rate of 5 m Vs^{-1} in LiCl aqueous electrolyte. The flexible solid state supercapacitor based on the symmetric ZnS-CT electrodes exhibits a specific capacitance of 540 F g^{-1} (areal capacitance of 56.25 F cm^{-2}), at scan rate of 5 m Vs^{-1} with excellent cycling stability. The high energy density of 51 Wh kg^{-1} at power density of 205 W kg^{-1} is achieved. Furthermore, three charged supercapacitors connected in series could light 4 red color light emitting diodes (2.0 V, 15 mA) for 2 min. ZnS nanospheres with large specific surface area combined with flexible carbon textile substrate offers a great prospect for energy storage devices with high energy.

2. Experimental Section

2.1 Materials

Carbon textile (thickness 0.2 mm) was purchased from Shanghai Lishuo Composite Material Technology Company. All other chemicals were of analytical grade and used without any further purification.

2.2. Synthesis of ZnS nanospheres on carbon textile

Carbon textile (CT) was used as a substrate, and ZnS nanospheres assembled on the CT was fabricated via a cost effective and simple hydrothermal method. Typically, first, a piece of CT was cut into desired size and treated with deionized water, acetone and absolute ethanol in sequence under sonication. The well-cleaned CTs were immersed in 0.25 M of zinc acetate solution and heated in air at 300 ^{o}C for 20 min, this process was repeated 3 times to form ZnO seeds on CT. Then pieces of prepared CTs stood on the wall of Teflon-lined stainless steel autoclave, which contains the reaction solution. The reaction solution is the mixture of zinc chloride ($ZnCl_2$) and potassium thiocyanate (KSCN) in ratio of 1:2 respectively, in 50 mL deionized water. After sealing, the autoclave was put into preheated electric furnace of 190 ^{o}C for 20 h. After the reaction, the autoclave was allowed to cool down to room temperature naturally, and then ZnS assembled CTs and the remaining off-white precipitates in the solution were washed with deionized water and ethanol. The ZnS assembled CTs and the filtered product from the solution was put into oven for 24 hours at 60 ^{o}C for drying. The ZnS assembled CTs were calcined at 350 ^{o}C for 1 h for the final fabrication of supercapacitor devices. The optical photographs of bare, ZnS assembled CTs before and after annealing are shown in Figure S1†and the schematic diagram of the fabrication process of ZnS assembled carbon textile with annealing process is shown in Figure S2†.

2.3. Fabrication of electrode and full-solid state supercapacitor

To check the pseudocapacitive behavior, the electrochemical performance of ZnS nanospheres assembled carbon textiles (ZnS-CT) is first characterized in three-electrode system with 6 M LiCl aqueous electrolyte. The ZnS-CT with working area of 2 × 2 cm^{-2} is used as working electrode, platinum foil as a counter electrode and Ag/AgCl as a reference electrode. The mass of active material on the CT is about 0.20 mg cm^{-2}. Further we fabricate the symmetric supercapacitors based on the ZnS-CTs. Positive and negative electrodes were the same of ZnS-CT with equal mass density and dimension (4.8 × 2 cm^2). The ZnS mass loading density on the CT is approximately 1.22 mg cm^{-2} carefully weighted by electronic balance. The flexible supercapacitors were assembled with two pieces of electrodes face-to-face separated by a solid state electrolyte (LiCl-PVA gel) and a separator (Whatman 8 μm filter paper). After being solidified at room temperature for 24 h, the prepared supercapacitor is ready for electrochemical testing.

2.4. Characterization and Electrochemical Measurement

The chemical composition and crystal structure of the prepared ZnS was characterized by X-ray diffraction (XRD) (PANalyticalX'Pert Powder with Cu Kα radiation). The morphology of the prepared sample was investigated by field emission scanning electron microscopy (FEI Nova 400 FEG-SEM). The specific surface area was measured by the multipoint Brunauer-Emmett-Teller (BET) method with Quadrasorb 2MP system and the pore size distribution was obtained by Barrett-Joyner-Halenda (BJH) method with Quantachrome Instrument (version 5.12). The cyclic voltammetry (CV) and galvanic charge-discharge (GCD) measurements were conducted using an electrochemical workstation (CHI 660D). The electrochemical impedance spectroscopy

(EIS) was carried out at 0.2 V amplitude in a frequency range of 0.01-100 kHz at open circuit potential.

3. Results and discussion

X-ray powder diffraction (XRD) pattern for the synthesized ZnS nanospheres is illustrated in Fig 1. To avoid the intense peaks of carbon textile, we performed the XRD analysis of the powder sample without carbon textile. All diffraction peaks could be easily indexed by the standard PDF No: 05-0566 with cubic structure. No impurities or residues have been detected, indicating the high purity of the synthesized product. The intense and sharp diffraction peaks confirm that the product is highly crystalline in nature.

The microstructure and morphology of the bare CT and ZnS-CT are shown in Figure 2. Figure 2A demonstrates the SEM image of the bare CT in which the intercrossed carbon fibers makes the 3D porous structure. Figure 2B shows the low resolution SEM image of the ZnS-CT, which indicates that the solid ZnS spheres are uniformly growing on the fibers of carbon textile. Inset of Figure 2B shows the photograph of the ZnS-CT and reveals the coverage of ZnS. Figure 2C clearly shows the ZnS nanospheres on a single fiber of carbon textile with high density with average diameter of 300-600 nm, which is further confirmed by the high resolution SEM image in Figure 2D. As the electrochemical performance of the supercapacitor depends on morphology of the electrode material, the high exposed active surface area of the ZnS spheres in the electrolyte can provide easy and fast transportation of electrolyte ions which would lead to the excellent electrochemical performance of the supercapacitor.

The specific surface area and porosity of the prepared ZnS spheres are investigated by N_2 adsorption and desorption measurement. Brunauer–Emmett–Teller (BET) surface area of ZnS

nanospheres was calculated as 28.5 m^2 g^{-1}. The pore size was calculated by N_2 adsorption and desorption isotherm using the Barrett–Joyner–Halenda (BJH) method and is shown in Figure S3 (A). A distinct hysteresis loop is observed which represents the typical type IV sorption behavior and indicates the existence of both nanopores and mesopores in the structure of the material. The average pore diameter of ZnS spheres is in nanoporous region. The maximum pore size of the sample is mostly in the range of 10-30 nm, as is shown in Figure S3(B). The linear increase in N_2 absorption at low pressure range (P/Po, 0.0-0.5) indicates the monolayer gas adsorption inside the pores. The sharp increase in N_2 in adsorption curve at high pressure range (P/Po, 0.7-1.0,) is due to the presence of interlayer spaces. Such a porous structure is considered as better energy storage due to high surface area and multi channels for ion diffusion since electron transportation and ion diffusion are two key factors for the enhancement of the electrochemical performance of the supercapacitor. Therefore the ZnS-CT supercapacitor may achieve the excellent performance due to its short ion diffusion and fast electron transportation from the 3D architecture of carbon textile assembled with ZnS spheres.

On the basis of above physical characterization, it is expected that the ZnS spheres assembled flexible carbon textile would have good electrochemical performance as a supercapacitor. First we carried out cyclic voltammetry (CV) and galvanostatic charge-discharge (GCD) measurements in 6 M LiCl aqueous solution in three electrode systems at room temperature. The CV curves for the ZnS-CT electrode at different scan rates from 5 to 75 m Vs^{-1} in potential window of -0.6 to 0.6 V are shown in Figure S4 (A). The specific capacitances are 747, 593.5, 431.8, 335 and 253.6 F g^{-1} at the scan rate of 5, 10, 25, 50 and 75 m Vs^{-1} respectively in 6 M LiCl liquid electrolyte is shown in Figure S4 (B). The GDC curves for ZnS-CT electrode at different current densities at potential window of 0 to 0.5 V are shown in Figure S4 (C)†. The

charging and discharging profile indicates good capacitive characteristics and they are in agreement with CV curves. The CV and GDC results are similar with the MnO_2[30] pseudocapacitive material. The good electrochemical performance of electrode is further confirmed from EIS spectra in Figure S4 (D). The ZnS-CT electrode has small internal resistance of 1.66 Ω. All above results of a single electrode demonstrate the pseudocapacitive features of ZnS spheres, making it a promising material for energy storage applications.

Secondly, the symmetric supercapacitor based on the ZnS-CTs was fabricated and the electrochemical performance was measured. Figure 3A and 3B shows the cyclic voltammetry (CV) curves of ZnS-CT supercapacitor at different scan rates ranging from 5 to 300 m Vs^{-1} in potential window of -0.8 to 0.8 V. The CV curves are close to ideal rectangular shape indicating excellent capacitive behavior and they display a similar behavior without any redox peaks, indicating that the ZnS-CT supercapacitor is charged and discharged at pseudo-constant rate over the entire voltammetric cycles.[31-32] The CV curve for the bare CT based supercapacitor at 50 m Vs^{-1} is also illustrated for comparison, demonstrating a negligible capacitive contribution, as is shown in Figure S5 (A). The CV curves are almost symmetric on voltage reversal from 0 to -0.8 V and from 0 to 0.8 V, as is shown in Figure 3C. The shape of CV curve remains in rectangular shape even at high scan rate of 300 m Vs^{-1} suggesting ideal electrochemical capacitive behavior. The specific capacitance C calculated from CV curves (detail calculation in Supporting Information) gives the highest specific capacitance of 540 F g^{-1} at scan rate of 5 m Vs^{-1} and 305 F g^{-1} at scan rate of 75 m Vs^{-1}. The highest areal capacitance of 56.25 F cm^{-2} at scan rate of 5 m Vs^{-1} and 15.62 F cm^{-2} at high scan rate of 250 m Vs^{-1} is achieved. The peak current density is directly proportional to the square root of the scan rate, as is shown in Figure S5 (B), which demonstrates fast electron transmission. The large specific capacitance is attributed to the high

exposed active surface area of the ZnS spheres to the electrolyte, which provides easy and fast transportation of Li^+ ions, as well as good contact of the ZnS spheres on the carbon textile which gives the fast electron transmission to the electrode. The decrease in capacitance at higher scan rates is due to the less diffusion of electrolyte ions (Li^+) into the interior surface of the active material of the electrode.[33]

Rate capability is an important factor in the evaluation of the performance of the supercapacitor. The galvanostatic charge-discharge (GCD) curves of ZnS-CT supercapacitor at different current densities ranging from 0.1 to 0.7 mA cm^{-2} in potential window of 0 to 1.0 V are shown in Figure 3E. All GCD curves have symmetrical and almost linear profiles suggesting high coulombic efficiency and good capacitive behavior. There is existence of small potential drop (*IR* drop) about 0.012 V at the beginning of the discharge cycle and it is also observed that *IR* drop increases with the increase in current density. The *IR* drop as a function of current density is shown in Figure S6, revealing that the electrode material has small ohmic resistance. At high current of 0.7 mA cm^{-2} the *IR* drop is only 0.11 V which demonstrate good conductivity of the carbon textile and a smaller internal resistance of the electrolyte. The electrode material with good electrical conductivity and high specific surface area exhibits excellent capacitive behavior.

For deeper understanding of the electrochemical performance, EIS is performed and results are presented in Figure 3F. The measured EIS spectra is analyzed using Nyquist plot and ZSimWin software simulation method based on equivalent electrical circuit, which is also shown in above inset of Figure 3F. The EIS spectra have a semicircle at high frequency region and a straight line at low frequency region. The straight line nearly parallels imaginary axis indicating good capacitive behavior. At high frequency part the intersection of the curve with real axis demonstrates the resistance of the electrochemical system (R_s~ 3.37Ω, which includes the ionic

resistance, contact resistance of electrode-electrolyte and inherent resistance of the material) and the diameter of semicircle represents the charge transfer resistance (R_{ct}~ 4.8 Ω). The smaller values of R_s and R_{ct} are indication of good electrical conductivity and electroactivity of the electrode material.[11, 29]

Figure 4A shows the CV curves of the ZnS-CT supercapacitor at a constant scan rate of 75 m Vs^{-1} in different operation potential windows. The CV curves attain the same rectangular shape indicating good stability of the supercapacitor. With the increase in operation potential window sharp increase in current is observed at higher potentials (1.5-1.6 V), demonstrating good capacitive behavior, as is shown in Figure 4B. The shape of the CV curves does not significantly change at higher voltage window of 1.6 V indicating excellent reversibility of the supercapacitor at constant scan rate of 75 m Vs^{-1}. The GDC curves of the ZnS-CT supercapacitor in different operation voltage windows ranging from 0.4 to 1.2 V at constant discharge current density of 0.5 mA cm^{-2} are shown in Figure 4C. The charging curves of the supercapacitor follows the same path up to even at high voltage of 1.2 V, demonstrating the stable charging-discharging profile and good capacitance characteristics of the ZnS-CT supercapacitor at high operating voltage.

For actual applications, flexible, thin, light weight and easily portable electronic devices are highly desired. The ZnS-CT supercapacitor is light weight, thin (0.85 g as a whole device including electrodes, electrolyte and separator, thickness 1.13 mm) and highly flexible and can be twisted at any angle without damaging its physical shape and performance, as is shown in Figure 6A. To evaluate its potential applications as a flexible energy storage device the electrochemical performance was checked under various bending conditions. The CV and GDC curves of the ZnS-CT supercapacitor twisted at different angles (flat, 45^o, 90^o, 180^o) are shown in

Figure 6B and 6C respectively, demonstrating no apparent change. These results indicate that the fabricated device is highly flexible.

Life span is very important factor for supercapacitors. The CV, GDC and EIS before and after long term (5000 cycles) are shown in Figure 6. The results demonstrate there is no significant loss in the performance of the supercapacitor. From EIS test, the small increase in the R_s (4.3 Ω, increase ~ 0.93Ω) might be due to the delamination of active material after long-term running. Thus, the ZnS-CT supercapacitor shows high electrochemical stability and rate capability for long cycle life applications.

The long-term cycling performance (number of cycles vs. capacitance retention) of the ZnS-CT supercapacitor is shown in Figure 7A. It is observed that the specific capacitance slightly decreases until first 3000 cycles and then increases and attains 94.6 % of its initial value at the end of 5000 cycles at constant current density of 0.8 mA cm^{-2}. The inset Figure 7A presents the charge-discharge process for the ZnS-CT supercapacitor, demonstrating excellent stability due to the high specific surface area of the ZnS spheres and good electrical conductivity between the spheres and CT.

The energy and power densities are calculated respectively (Supporting Information). The Ragone plot of the calculated specific energy and specific power at different current densities are shown in Figure 7B. The ZnS-CT symmetric supercapacitor exhibits a high energy density of 51 Wh kg^{-1} at power density of 205 W kg^{-1} and even at high power density of 822 W kg^{-1} the supercapacitor have an energy density of 22.66 Wh kg^{-1}, much superior to TMOs and TMCs based symmetric supercapacitors. The detailed comparison of the current work with previous literatures is presented in table 1.

Table 1: The comparison of the ZnS-CT based single electrode and full solid state supercapacitor with previous literatures, where we denote C_{SS} for Specific Capacitance (Single electrode), C_{ST} for Specific Capacitance (two electrode device), v for scan rate, n for cycle numbers, E for Energy density and P for Power density.

No	Materials	C_{SS} (F g^{-1}) at v (mVs^{-1})	C_{ST} (F g^{-1}) at v (mVs^{-1})	E (Wh kg^{-1})	P (W kg^{-1})	Stability (%) after n	Ref.
0	ZnS nanospheres	747 at 5 mVs^{-1}	540 at 5 mVs^{-1}	51	205	94.6, 5000	This work
1	Cu_7S_4 Nanowires		400 at 10 mVs^{-1}	35	200	95, 5000	11
2	KCu_4Se_8/V_2O_5 Nanowires		93.7 at 5 mVs^{-1}	1.7	8.3	37.4, 5000	12
3	MoS_2 Nanospheres		368 at 5 mVs^{-1}	5.42	128	96.5, 5000	13
4	Co_9S_8 Nanoflakes		82.9 1 A/g	31.4	200	90, 5000	15
5	Hybrid ZnO/ZnS	0.217 F cm^{-2} at 1 mA cm^{-2}		-	-	82, 2000	22
6	ZnO@MnO_2	423.5 at 0.5 A/g		-	-	92, 3000	34
7	$ZnMn_2O_4$	160 at 3 mVs^{-1}		18	185	-	35
8	3D ZnO@MnO_2	537.8 at 5 mVs^{-1}		-	-	89.8, 5000	36
9	ZnO-Activated carbon	178.2 at 1 mA cm^{-2}		22.71	400	75, 1000	37
10	Zn-graphene composite	61.7 at 5 mVs^{-1}		-	-	90, 100	38
11	$NiMoO_4.xH_2O$		96.7 at 5 mA cm^{-2}	34.4	165	80.6, 1000	39
12	$NiWO_4$ Nanostructures		71.1 at 0.25 A/g	25.3	200	91.4, 5000	40

The high energy and power densities of the ZnS-CT supercapacitor are attributed to the following factors: (1) the electron transportation is significantly enhanced by the direct growth of active materials on conductive carbon textile. (2) The 3D nano-micro spheres provide porous channels for deeper penetration of electrolyte ions and enhance the specific capacitance. (3) The low internal resistance of the ZnS-CT electrodes provides a high charge transfer rate between the active material and electrolyte (which has only a slight increase (0.93 Ω) in internal resistance after 5000 cycles). (4) Direct growth architectures on conductive substrates ensure the good physical adhesion, electrical conductivity and stability of the active material. (5) The active materials growing directly on a conductive carbon textile also avoids the use of conductive agents and polymer binders which may increase the resistance of the materials. These features result in the high electrochemical performance of the ZnS-CT supercapacitor.

For practical applications, three supercapacitors in series can be easily charged up to 3 V, as is shown in Figure 8A. Three charged supercapacitors in series can light 4 red color LED's (2.0 V, 15 mA) for 2 min. The optical photograph of lighted LED's is shown in Figure 8B demonstrating its capability as a good storage device.

Conclusions

An easy and cost effective method for the fabrication of ZnS nanospheres on conductive carbon textile for electrodes of high performance solid state flexible supercapacitor is reported. The fabricated ZnS-CT supercapacitor shows excellent electrochemical performance along with light weight and good flexibility. The ZnS-CT supercapacitor demonstrates good capacitive behavior with high specific capacitance of 540 F g^{-1} and areal capacitance of 56.25 F cm^{-2} at scan rate of 5 m Vs^{-1} with good rate capability and excellent cycling stability (94.6 % retention of initial

capacitance after 5000 cycles). High energy density of 51 Wh kg^{-1} at power density of 205 W kg^{-1} is achieved. These results suggest that the ZnS-spheres growing directly on a carbon textile is a promising material for supercapacitor applications.

Acknowledgments

This work is supported by the National High Technology Research and Development Program (863 program) of China (2015AA034801), Chongqing University Postgraduates' Innovation Project (CYB15044), NSFCQ (cstc2015jcyjA20020, cstc2012jjA50024), The Science and Technology Research Project of Chongqing Municipal Education Commission of China (KJ130603, KJKJ1400607).

1. M. Conte, Fuel Cells, 2010, 10, 806-828.
2. P. Yang and W. Mai, *Nano Energy*, 2014, **8**, 274-290.
3. M. Winter and R. J. Brodd, *Chem. Rev.*, 2004, **104**, 4245-4270.
4. J. Zhong, Y. Zhang, Q. Zhong, Q. Hu, B. Hu, Z. L. Wang and J. Zhou, *ACS nano*, 2014, 8, 6273-6280.
5. X. Sun, H. Sun, H. Li and H. Peng, *Adv. Mater.*, 2013, **25**, 5153-5176.
6. X. Huang, Z. Zeng, Z. Fan, J. Liu and H. Zhang, *Adv.Mater.*, 2012, **24**, 5979-6004.
7. F. Wang, S. Xiao, Y. Hou, C. Hu, L. Liu and Y. Wu, *Rsc Adv.*, 2013, **3**, 13059-13084.
8. M.-R. Gao, Y.-F. Xu, J. Jiang and S.-H. Yu, *Chem. Soc. Rev.*, 2013, **42**, 2986-3017.
9. J. Jiang, Y. Li, J. Liu, X. Huang, C. Yuan and X. W. D. Lou, *Adv. Mater.*, 2012, **24**, 5166-5180.
10. X. Lu, M. Yu, G. Wang, Y. Tong and Y. Li, *Energy Environ. Sci.*, 2014, **7**, 2160- 2181.
11. M. S. Javed, S. Dai, M. Wang, Y. Xi, Q. Leng, D. Guo and C. Hu, *Nanoscale*, 2015, 7, 13610-13618.
12. K. Zhang, H. Chen, X. Wang, D. Guo, C. Hu, S. Wang, J. Sun and Q. Leng, *J. Power Sources*, 2014, **268**, 522-532.
13. M. S. Javed, S. Dai, M. Wang, D. Guo, L. Chen, X. Wang, C. Hu and Y. Xi, *J. Power Sources*, 2015, **285**, 63- 69.
14. H. Pang, C. Wei, X. Li, G. Li, Y. Ma, S. Li, J. Chen and J. Zhang, *Sci. Rep.*, 2014, **4,** 1-8.
15. R. Rakhi, N. A. Alhebshi, D. Anjum and H. Alshareef, *J. Mater. Chem. A*, 2014, **2**, 16190- 2567.
16. S. Ratha and C. S. Rout, *ACS App.Mater.Inter.*, 2013, **5**, 11427- 11433.
17. X. Rui, H. Tan and Q. Yan, *Nanoscale*, 2014, **6**, 9889-9924.

18. X. Fang, T. Zhai, U. K. Gautam, L. Li, L. Wu, Y. Bando and D. Golberg, *Prog. Mater. Sci.,* 2011, **56**, 175-287.

19. J. K. Kim, S. Bae, W. Kim, M. J. Jeong, S. H. Lee, C.-L. Lee, W. K. Choi, J. Y. Hwang, J. H. Park and D. I. Son, *Nano Energy*, 2015, **13**, 258-266.

20. X. Gu, S. Zhang, Y. Zhao and Y. Qiang, *Vacuum*, 2015, **122, Part A**, 6-11.

21. X. Wang, P. Gao, J. Li, C. J. Summers and Z. L. Wang, *Adv. Mater*, 2002, **14**, 1-3.

22. S. Zhang, B. Yin, H. Jiang, F. Qu, A. Umar and X. Wu, *Dal. Trans.*, 2015, **44**, 2409, - 2415.

23. B. Guan, D. Guo, L. Hu, G. Zhang, T. Fu, W. Ren, J. Li and Q. Li, *J. Mater.Chem. A*, 2014, **2**, 16116-16123.

24. M. Sawangphruk, M. Suksomboon, K. Kongsupornsak, J. Khuntilo, P. Srimuk, Y. Sanguansak, P. Klunbud, P. Suktha and P. Chiochan, *J. Mater.Chem. A*, 2013, **1**, 9630 - 9636.

25. Y. Chen, X. Zhang, H. Zhang, X. Sun, D. Zhang and Y. Ma, *RSC Adv.*, 2012, **2**, 7747-7753.

26. D. Guo, P. Zhang, H. Zhang, X. Yu, J. Zhu, Q. Li and T. Wang, *J. Mater.Chem. A*, 2013, **1**, 9024-9027.

27. C. Dong, Y. Wang, J. Xu, G. Cheng, W. Yang, T. Kou, Z. Zhang and Y. Ding, *J.Mater.Chem. A*, 2014, **2**, 18229-18235.

28. N. Yu, M.-Q. Zhu and D. Chen, *J.Mater.Chem. A*, 2015, **3**, 7910-7918.

29. D. Guo, Y. Luo, X. Yu, Q. Li and T. Wang, *Nano Energy*, 2014, **8**, 174-182.

30. P. Yu, X. Zhang, D. Wang, L. Wang and Y. Ma, *Cryst. Grow.Desi.*, 2008, **9**, 528 -533.

31. L.-F. Chen, Z.-Y. Yu, J.-J. Wang, Q.-X. Li, Z.-Q. Tan, Y.-W. Zhu and S.-H. Yu, *Nano Energy*, 2015, **11**, 119-128.

32. W. Zhou, X. Liu, Y. Sang, Z. Zhao, K. Zhou, H. Liu and S. Chen, *ACS App. Mater. Inter.*, 2014, 6, 4578-4586.

33. Y. Han, Y. Wang, W. Gao, Y. Wang, L. Jiao, H. Yuan and S. Liu, *Powd. Tec.*, 2011, **212**, 64-68.

34. M. Huang, F. Li, X. L. Zhao, D. Luo, X. Q. You, Y. X. Zhang and G. Li, *Electrochim. Acta*, 2015, **152**, 172-177.

35. A. Sahoo and Y. Sharma, *Mater. Chem.Phy.*, 2015, **149**, 721-727

36. C. Yuan, H. Lin, H. Lu, E. Xing, Y. Zhang and B. Xie, *Energy*, 2015, **93, Part 2**, 1259-1266.

37 C. H. Kim and B.-H. Kim, *J.Power Sources*, 2015, **274**, 512-520

38. T. Lu, Y. Zhang, H. Li, L. Pan, Y. Li and Z. Sun, *Electrochimica Acta*, 2010, **55**, 4170-4173.

39. M.-C. Liu, L. Kang, L.-B. Kong, C. Lu, X.-J. Ma, X.-M. Li and Y.-C. Luo, *RSC Adv.*, 2013, **3**, 6472-6478.

40. L. Niu, Z. Li, Y. Xu, J. Sun, W. Hong, X. Liu, J. Wang and S. Yang, *ACS App.Mater.Inter.*, 2013, **5**, 8044-8052.

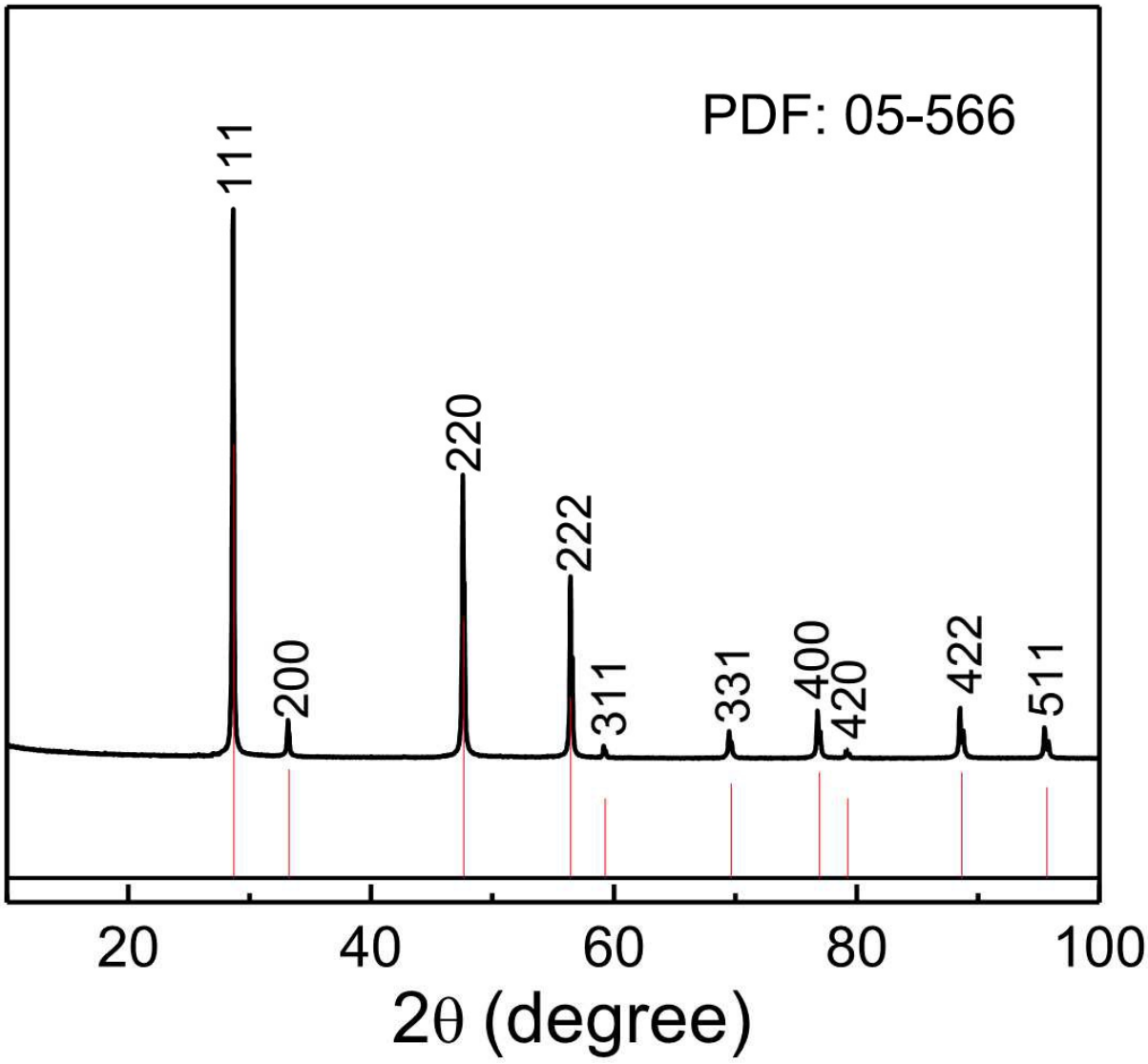

Figure 1. XRD pattern of synthesized ZnS nanospheres.

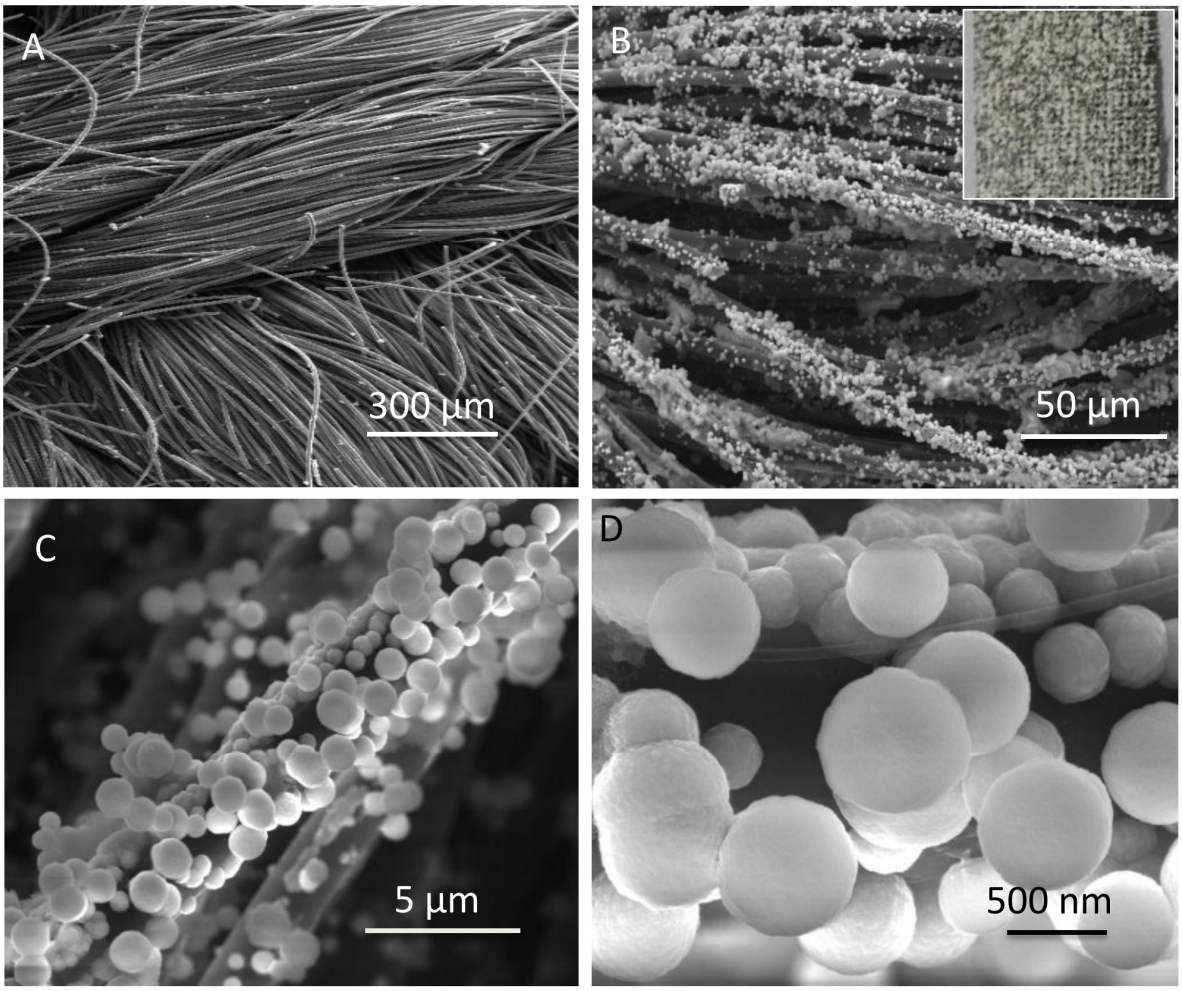

Figure 2. SEM images of the synthesized ZnS nanospheres at different magnifications. (A) Bare carbon textile, (B) ZnS nanospheres growing on carbon textile, (C) and (D) ZnS nanospheres growing on single fiber of carbon textile.

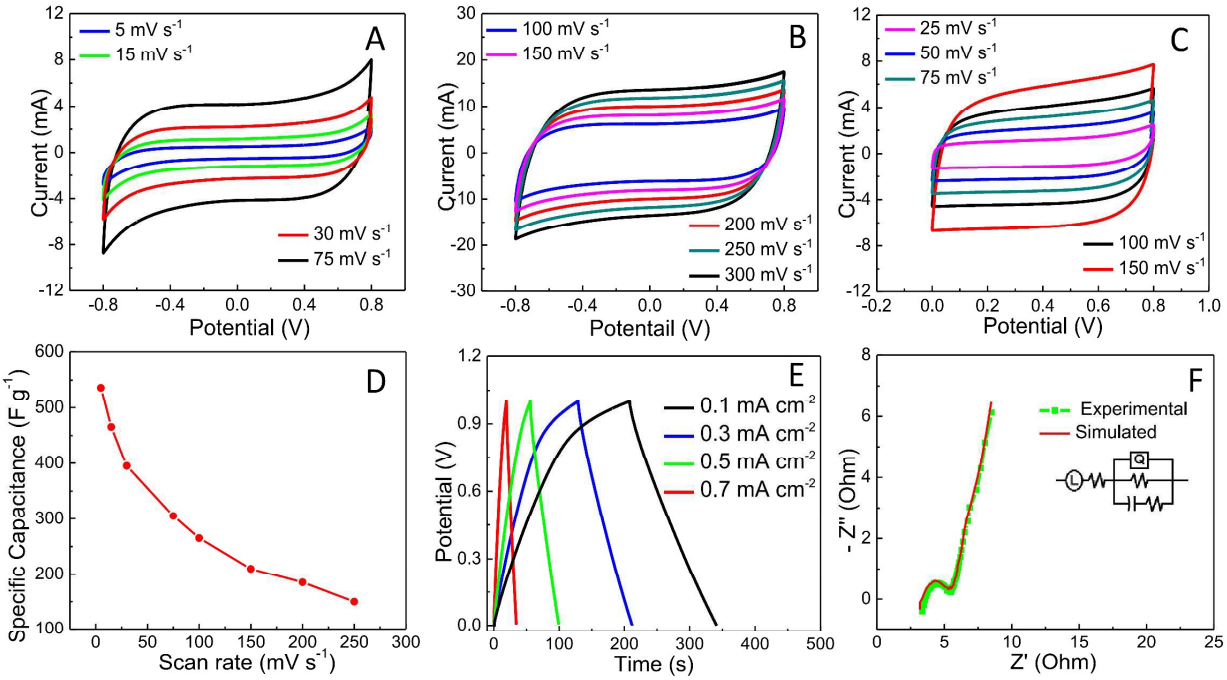

Figure 3. Electrochemical performances of the ZnS-CT solid state supercapacitor (A and B) CV curves at different scan rates ranging from 5 to 300 m Vs^{-1} in potential window of -0.8 to 0.8 V, (C) CV curves at different scan rates ranging from 25 to 150 m Vs^{-1} in potential window of 0 to 0.8 V, (D) specific capacitance as a function of scan rate, (E) charging-discharging curves taken at different current densities ranging from 0.1 to 0.7 mA cm^{-2} in potential window of 0 to 1 V, (F) Nyquist plot of impedance from 0.01 to 100 kHz, inset is the corresponding equivalent electrical circuit.

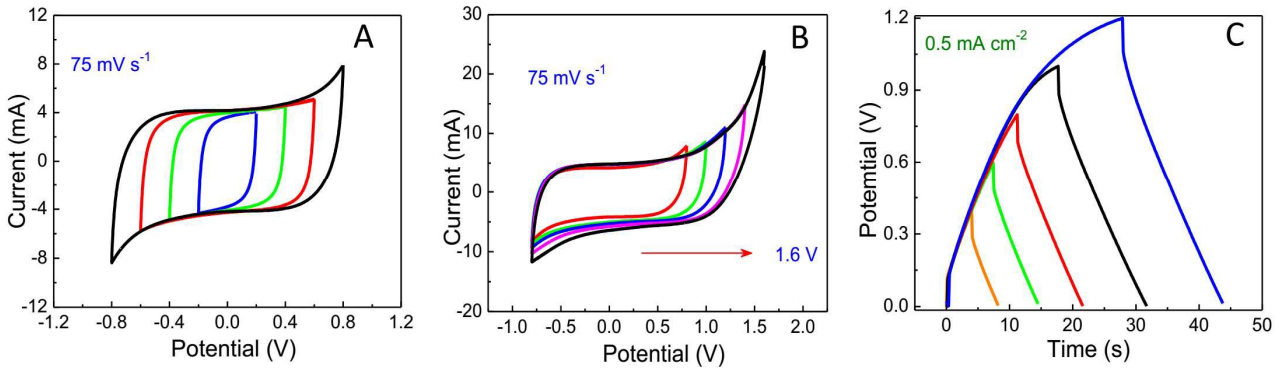

Figure 4. Electrochemical performance of ZnS-CT solid state supercapacitor (A) CV curves at constant scan of 75 m Vs^{-1} in different potential windows ranging from -0.8 to 0.8, (B) CV curves at different potential windows from -0.8 to 1.6 V at constant scan rate of 75 m Vs^{-1}, (C) Charging-discharging curves taken at current density of 0.5 mA cm^{-2} at different potential windows ranging from 0.4 to 1.2 V.

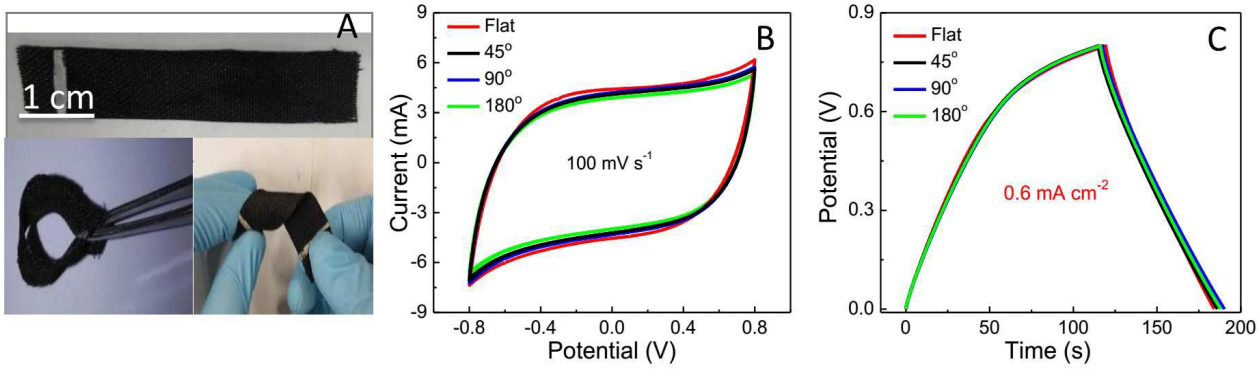

Figure 5. Performance of ZnS-CT solid state supercapacitor at different bending angles, the bent device has no effect on its performance as seen in (A) digital photographs of solid state supercapacitor bent in different angles showing the flexibility of the device, (B) CV curves at a scan rate of 100 mV s^{-1}, (C) charging-discharging curves taken at 0.6 mA cm^{-2}.

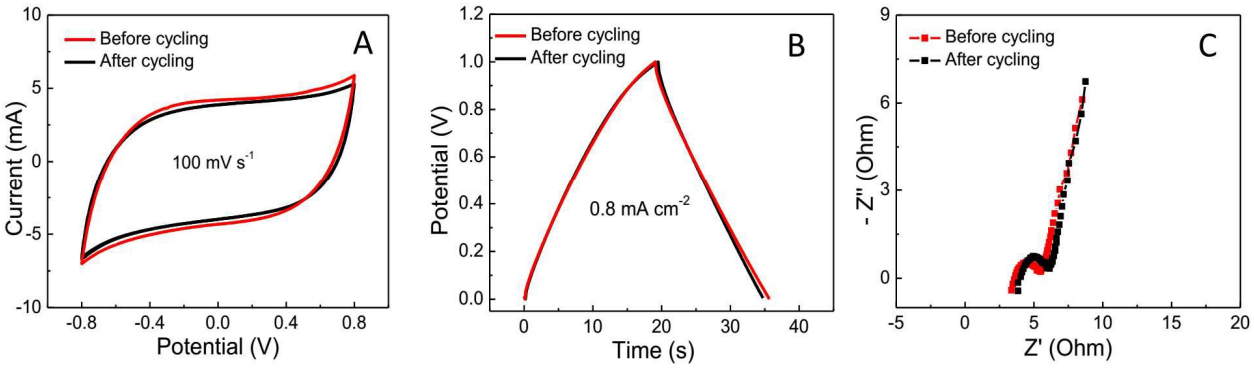

Figure 6. Long term cycling performance of ZnS-CT solid state supercapacitor (A) CV curves before and after 5000 cycles at scan rate of 100 mV s^{-1}, (B) charging-discharging curves before and after 5000 cycles taken at current density of 0.8 mA cm^{-2}, (C) EIS spectra before and after 5000 charging discharging cycles.

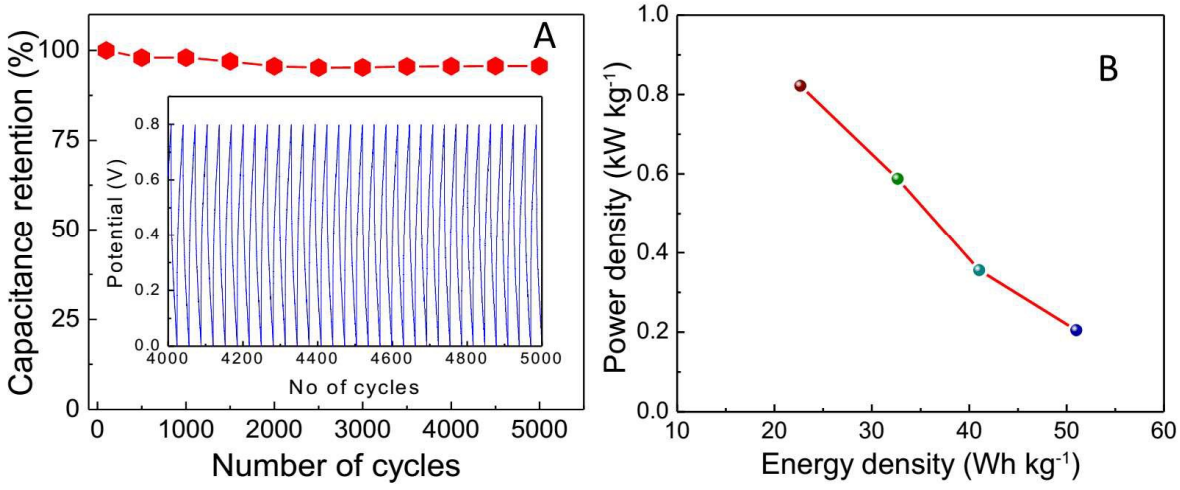

Figure 7. (A) Cyclic performance of ZnS-CT solid state supercapacitor at constant current density of 0.8 mA cm^{-2}, the inset shows charge-discharge in potential window of 0 to 0.8 V at 0.1 mA cm^{-2}. (B) Ragone plot (Energy density vs. Power density) of the supercapacitor.

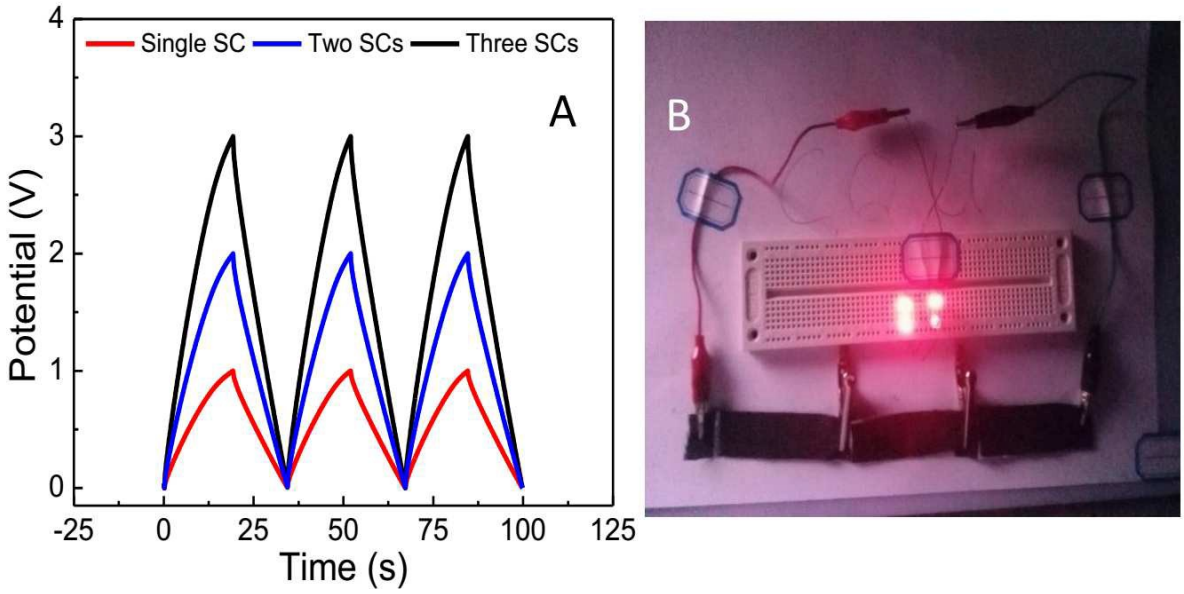

Figure 8. (A) Charging-discharging curves of ZnS-CT supercapacitor device at constant current density of 0.5 mA cm^{-2}, Single device can charge up to 1 V, two devices in series can charge up to 2 V and three devices in series can charge up to 3 V, (B) Three charged supercapacitors connected in series could lit the 4 red color LEDs.

Graphical Abstract

A large number of pores between the spheres provide channels to let electrolyte ions reach easily to the reaction sites, while the carbon textile provides the easy transportation of electrons. The well-organized spheres with large interfaces create more active sites which lead the efficient insertion-extraction of electrolyte ions into the active material to enhance the electrochemical performance.